Journal of Applied Mechanics and Technical Physics, Vol. 44, No. 5, pp. 736–740, 2003

DIFFRACTION OF SURFACE WAVES BY THE EDGE OF A WEDGE

S. Yu. Gurevich and Kh. B. Tolipov

UDC 539.25

Conditions of propagation of Rayleigh waves over an elastic wedge are considered. Refraction factors are determined for conversion of the initial wave into secondary volume and surface waves. Calculation results for the modules of the refraction coefficient agree well with published experimental data.

Key words: *diffraction, Rayleigh wave, Fourier transform, longitudinal and transverse potentials.*

Introduction. Diffraction of surface (Rayleigh) waves by a wedge has a wide range of applications (for example, in converters of surface waves to volume waves, in elimination of false signals in delay circuits, etc).

The mechanism of diffraction of surface waves can be described quite simply. A wave propagating over one face of a wedge generates an inhomogeneous perturbation of the other face on a length l. The magnitude and shape of the perturbation depend on the wedge angle and the depth of the Rayleigh wave (see Fig. 1, where W_1 is the incident wave and W_2 is the refracted wave). This perturbation is a source of secondary waves, which, on the boundary of the face, can be mathematically expressed as a spectrum of spatial Fourier harmonics. Harmonics with wave numbers $k = k_{\mathrm{R}}$ describe the Rayleigh wave field, whereas harmonics with wave numbers $k < k_{\mathrm{tr}}$ correspond to the volume wave field (k_{R} and k_{tr} are the wave numbers of the Rayleigh and shear waves, respectively).

1. Formulation of the Problem. We assume that a Rayleigh wave propagating over the first face of the wedge is a combination of two waves (Fig. 1): a longitudinal wave and a shear wave with the potentials

$$\Phi = \exp\left[i(k_{\mathrm{R}}\varepsilon - \omega t) - \sqrt{k_{\mathrm{R}}^2 - k_{\mathrm{long}}^2}\,\eta\right], \quad \Psi = p\exp\left[i(k_{\mathrm{R}}\varepsilon - \omega t) - \sqrt{k_{\mathrm{R}}^2 - k_{\mathrm{tr}}^2}\,\eta\right],$$

$$p = -\sqrt{\frac{k_{\mathrm{long}}^2 - k_{\mathrm{R}}^2}{k_{\mathrm{tr}}^2 - k_{\mathrm{R}}^2}}\,i, \quad k_{\mathrm{long}} = \frac{\omega}{c_{\mathrm{long}}}, \quad k_{\mathrm{tr}} = \frac{\omega}{c_{\mathrm{tr}}}, \quad k_{\mathrm{R}} = \frac{\omega}{c_{\mathrm{R}}}.$$

Here c_{long}, c_{tr}, and c_{R} are the velocities of the longitudinal, transverse, and Rayleigh waves, respectively, and ω is the angular rate. The amplitude of the longitudinal potential is set equal to unity. [Below, the time dependence $\exp(-i\omega t)$ is omitted.]

The time-dependent parts of the elastic fields generated by the incident Rayleigh wave on the other face of the wedge are described by the equations

$$\Delta\Phi + k_{\mathrm{long}}^2\Phi = 0, \qquad \Delta\Psi + k_{\mathrm{tr}}^2\Psi = 0. \tag{1}$$

As is known, the stress tensor components are calculated from the equations [1]

$$\sigma_{\tau\nu} = \mu\Big(2\,\frac{\partial^2\Phi}{\partial\tau\,\partial\nu} + \frac{\partial^2\Psi}{\partial\tau^2} - \frac{\partial^2\Psi}{\partial\nu^2}\Big), \qquad \sigma_{\nu\nu} = 2\mu\Big(-\frac{\partial^2\Phi}{\partial\tau^2} - \frac{k_{\mathrm{tr}}^2}{2}\,\Phi + \frac{\partial^2\Psi}{\partial\tau\,\partial\nu}\Big).$$

On the second face of the wedge, the stress tensor components induced by both the incident wave and its generated secondary waves should be equal to zero. If σ_{zz}^0 and σ_{xz}^0 are stresses induced by displacements of the incident Rayleigh wave, the boundary conditions for $z = 0$ are written as

$$\sigma_{zz} = -\sigma_{zz}^0, \qquad \sigma_{xz} = -\sigma_{xz}^0. \tag{2}$$

South Ural State University, Chelyabinsk 454080. Translated from Prikladnaya Mekhanika i Tekhnicheskaya Fizika, Vol. 44, No. 5, pp. 161–166, September–October, 2003. Original article submitted October 14, 2002; revision submitted January 20, 2003.

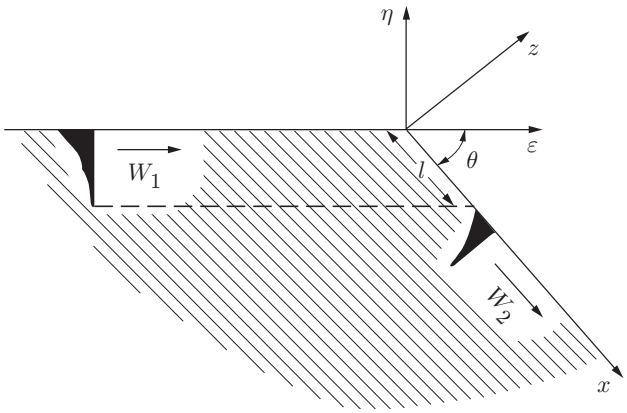

Fig. 1

The stresses induced by displacements of the Rayleigh wave on the first face of the wedge are written as [2]

$$\sigma_{\varepsilon\eta} = [P(k_{\mathrm{R}}) \exp{(i\sqrt{k_{\mathrm{long}}^2 - k_{\mathrm{R}}^2}\,\eta)} + Q(k_{\mathrm{R}}) \exp{(i\sqrt{k_{\mathrm{tr}}^2 - k_{\mathrm{R}}^2}\,\eta)}] \exp{(ik_{\mathrm{R}}\varepsilon)},$$

$$\sigma_{\eta\eta} = [R(k_{\mathrm{R}}) \exp{(i\sqrt{k_{\mathrm{long}}^2 - k_{\mathrm{R}}^2}\,\eta)} + S(k_{\mathrm{R}}) \exp{(i\sqrt{k_{\mathrm{tr}}^2 - k_{\mathrm{R}}^2}\,\eta)}] \exp{(ik_{\mathrm{R}}\varepsilon)},$$

where $P(k_{\mathrm{R}}) = 2k_r\sqrt{k_{\mathrm{long}}^2 - k_{\mathrm{R}}^2}$, $Q(k_{\mathrm{R}}) = 2k_{\mathrm{R}}^2 - k_{\mathrm{tr}}^2$, $R(k_{\mathrm{R}}) = -\lambda k_{\mathrm{long}}^2 - 2\mu(k_{\mathrm{R}}^2 - k_{\mathrm{tr}}^2)$, $S(k_{\mathrm{R}}) = 2k_{\mathrm{R}}\sqrt{k_{\mathrm{tr}}^2 - k_{\mathrm{R}}^2}$, and λ and μ are Lamé constants. We note that on the second face of the wedge, the value and direction of these stresses vary with variation in the wedge angle and Rayleigh wave depth.

We also assume that the wedge edge, which is the common boundary of the wedge faces, is not perturbed, and, hence, has no effect on the formation of the field. As is shown below, agreement between experimental and theoretical curves indicates the validity of the adopted assumption.

By virtue of the inhomogeneity of the Rayleigh wave, the projections of the longitudinal and shear components of the incident wave vector onto the x and z axes are written in complex form

$$k_{1x}(\theta) = k_{\mathrm{R}}\cos\theta + i\sqrt{k_{\mathrm{R}}^2 - k_{\mathrm{long}}^2}\sin\theta, \qquad k_{1z}(\theta) = k_{\mathrm{R}}\sin\theta + i\sqrt{k_{\mathrm{R}}^2 - k_{\mathrm{long}}^2}\cos\theta,$$

$$k_{2x}(\theta) = k_r\cos\theta + i\sqrt{k_{\mathrm{R}}^2 - k_{\mathrm{tr}}^2}\sin\theta, \qquad k_{2z}(\theta) = k_r\sin\theta + i\sqrt{k_{\mathrm{R}}^2 - k_{\mathrm{tr}}^2}\cos\theta.$$

In this case, for the potential field upon decomposition of the perturbing forces onto tangential and normal components, the boundary conditions on the second wedge face ($z = 0$) become

$$2\frac{\partial^2\Phi}{\partial x\,\partial z} + \frac{\partial^2\Psi}{\partial x^2} - \frac{\partial^2\Psi}{\partial z^2} = \sigma_1 + \sigma_2, \qquad -\frac{\partial^2\Phi}{\partial x^2} - \frac{k_{\mathrm{tr}}^2}{2}\Phi + \frac{\partial^2\Psi}{\partial x\,\partial z} = \sigma_3 + \sigma_4,$$

where

$$\sigma_1 = [P(k_{1x}) \exp{(ik_{1x}x)} + pQ(k_{2x}) \exp{(ik_{2x}x)}] \cos\theta,$$

$$\sigma_2 = [P(k_{1z}) \exp{(ik_{1z}z)} + pQ(k_{2z}) \exp{(ik_{2z}z)}] \sin\theta,$$

$$\sigma_3 = [R(k_{1x}) \exp{(ik_{1x}x)} + pS(k_{2x}) \exp{(ik_{2x}x)}] \cos\theta,$$

$$\sigma_4 = [R(k_{1z}) \exp{(ik_{1z}z)} + pS(k_{2z}) \exp{(ik_{2z}z)}] \sin\theta.$$

2. Construction of a Solution. We write the unknown solution as a Fourier transform in the coordinates x and z:

$$A_j^* = \int\limits_{-\infty}^{\infty} A_j(k,x) \exp{(ikx)}\,dx, \qquad C_j^* = \int\limits_{-\infty}^{\infty} A_j(k,z) \exp{(i(kz + 0.5\pi))}\,dz, \qquad j = 1,2,$$

$$A_1 = \Phi, \qquad A_2 = \Psi. \tag{3}$$

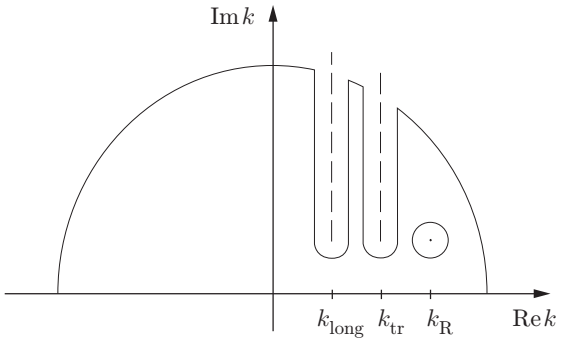

Fig. 2

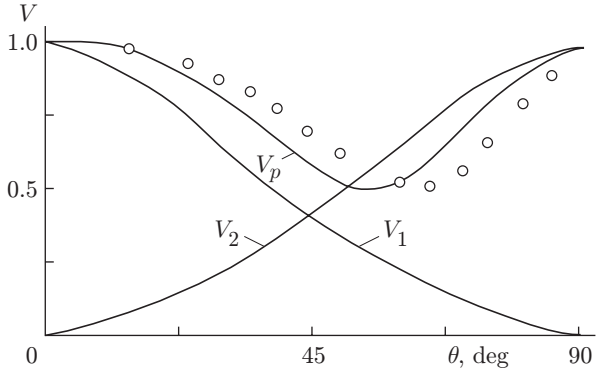

Fig. 3

The desired functions A_j^* and C_j^* are found by substitution of relations (3) into (1) and (2) and subsequent solution of the ordinary differential equations.

We first consider the solution for the case of tangential forces. Omitting simple computations, we finally obtain

$$A_1^* = T_1 \exp(iqz), \qquad C_1^* = T_2 \exp(iqz),$$

$$T_0 = 4k^2qs - (k^2+s^2)^2, \quad T_1 = (T_3+T_4)/T_0, \quad T_2 = (T_5+T_6)/T_0, \quad q^2 = k^2 - k_{\text{long}}^2, \quad s^2 = k^2 - k_{\text{tr}}^2,$$

$$T_3 = [B_1(\theta)S(k_{\text{R}}) - B_2(\theta)Q(k_{\text{R}})]\cos\theta, \qquad T_4 = [B_2(\theta)S(k_{\text{R}}) - B_2(\theta)Q(k_{\text{R}})]\sin\theta,$$

$$T_5 = [B_2(\theta)P(k_{\text{R}}) - B_1(\theta)R(k_{\text{R}})]\cos\theta, \qquad T_6 = [B_4(\theta)P(k_{\text{R}}) - B_3(\theta)R(k_{\text{R}})]\sin\theta, \tag{4}$$

$$B_1 = P(k_{1x})/(k-k_{1x}) - pQ(k_{2x})/(k-k_{2x}), \qquad B_2 = R(k_{1x})/(k-k_{1x}) - pS(k_{2x})/(k-k_{2x}),$$

$$B_3 = P(k_{1z})/(k-k_{1z}) - pQ(k_{2z})/(k-k_{2z}), \qquad B_4 = R(k_{1z})/(k-k_{1z}) - pS(k_{2z})/(k-k_{2z}).$$

3. Calculations of the Field of Rayleigh Wave Displacements. In the inverse Fourier transform, we continue the integrand analytically into the complex plane. In this plane, the integrand has the branching points

$$k_{1,2} = \pm ik_{\text{long}}, \qquad k_{3,4} = \pm ik_{\text{tr}}$$

and simple poles

$$k_{5,6} = \pm ik_{\text{R}}.$$

We choose the branches of the radicals in (4) from the condition $\arg q = \arg s = \pi/2$ for $k > 0$ and draw sections from the branching points along the lines $\text{Re}\,(q,s) = 0$.

To remove the singularities from the real axis ($-\infty < k < \infty$), we assume that there is weak attenuation in the medium, i.e., that k_{long} and k_{tr} are complex numbers.

We replace the integrals along the real axis by the integral along the path Γ that passes along this axis, arcs of a circle of infinite radius in the upper half-plane subtended by the real axis, and the banks of cuts passing through the branching points (Fig. 2). This integration contour was chosen because the integrand satisfies Jordan's lemma.

Thus, we can write

$$\int\limits_{-\infty}^{\infty} F(k) = \int\limits_{\Gamma} F(k) - \int\limits_{L} F(k) - \int\limits_{L_1} F(k) - \int\limits_{L_2} F(k) - \int\limits_{\gamma_{\text{long}}} F(k) - \int\limits_{\gamma_{\text{tr}}} F(k). \tag{5}$$

The integral along the path Γ is equal to the sum of residues taken over the poles enclosed in the integration contour.

In the case of tangential forces, the refraction coefficient is given by

$$V_1 = T_1 \Big(\frac{d}{dk} T_0(k)\Big|_{k=k_{\text{R}}} \Big)^{-1}.$$

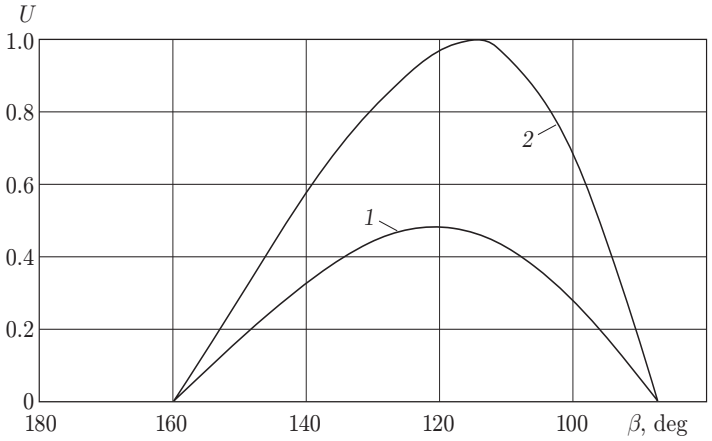

Fig. 4

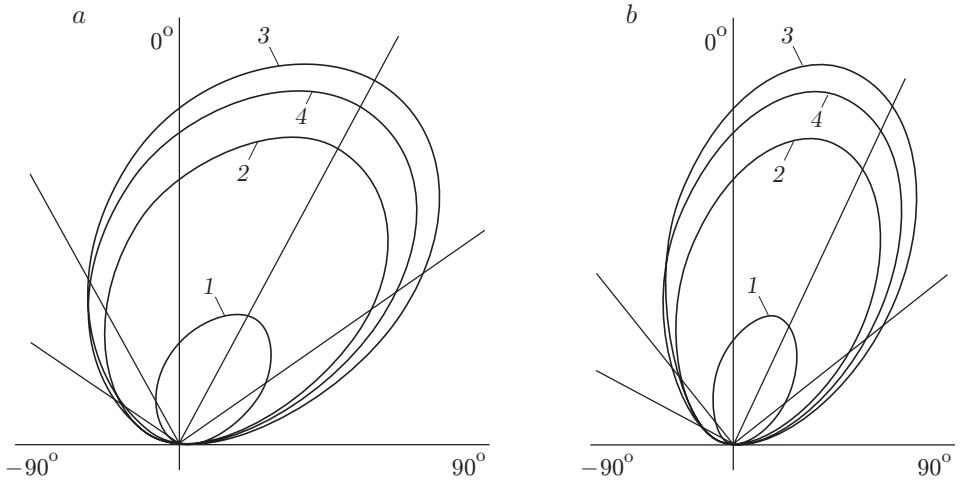

Fig. 5

Applying the above procedure to the refraction coefficient in the case of normal perturbations, we have

$$V_2 = T_2\Big(\frac{d}{dk}\,T_0(k)\Big|_{k=k_{\mathrm{R}}}\Big)^{-1}.$$

During wave propagation, the general refraction coefficient is written in complex form because the phase changes with respect to the incident wave:

$$|V_p|\mathrm{e}^{i\varphi} = V_1 + V_2.$$

Figure 3 shows calculation results for the modules of the refraction coefficients of the Rayleigh wave (curves) and experimental data (points) of [1].

An analysis shows that for large wedge angles, the tangential components of the perturbing forces make the major contribution to the scattered acoustic field. With increase in the angle θ, the contribution of these forces decreases, whereas the effect of the normal component, which monotonically reaches a maximum, increases. We also note that the experimental points are shifted to the right with respect to the calculated curve. This is explained by the following. According to the aforesaid, the conversion coefficient of surface waves decreases with variation in the wedge angle. If the projection of the incident wave vector onto the free surface exceeds the volume wave vector, the induced longitudinal and transverse waves are inhomogeneous, and their energy is entirely concentrated in the vicinity of the surface [3]. Consequently, for large wedge angles, the entire energy of the incident wave is converted to the energy of the refracted inhomogeneous wave, which is then converted to a Rayleigh wave. Thus, the conversion coefficient begins to decrease after the appearance of the volume wave, which carries the energy into

the depth of the medium [4]. This occurs when the projection of the incident wave vector onto the other face of the wedge is smaller than the shear wave vector. This condition is given by the relation $\theta_0 = \arccos(k_{\rm tr}/k_{\rm R})$. For the chosen material with Poisson's ratio $\sigma = 0.34$, we have $\theta_0 = 15^\circ$.

4. Calculation of the Displacement Field of Volume Waves. If the contours $\gamma_{\rm long}$ and $\gamma_{\rm tr}$ are drawn through the saddle points and the direction of circulation about the integration contour coincides with the direction of the fastest descent, the last terms in (5) are governing. Omitting simple calculations, we give the following relations for displacements of longitudinal and transverse waves

$$U_{\rm long} = \sqrt{\frac{2\pi}{k_{\rm long}\rho}}\,\frac{\cos^2\omega}{k_{\rm long}^3 D_{\rm long}}\Big[\Big(p\,\frac{2k_{2x}^2 - k_{\rm tr}^2}{k_{\rm long}\sin\omega - k_{2x}} - \frac{2k_{1x}\sqrt{k_{\rm long}^2 - k_{1x}^2}}{k_{\rm long}\sin\omega - k_{1x}}\Big)2k_{\rm R}\sqrt{k_{\rm R}^2 - k_{\rm tr}^2}$$

$$+\Big(p\,\frac{2k_{2x}\sqrt{k_{\rm tr}^2 - k_{2x}^2}}{k_{\rm long}\sin\omega - k_{2x}} + \frac{2k_{1x}^2 - k_{\rm tr}^2}{k_{\rm long}\sin\omega - k_{1x}}\Big)(2k_{\rm R}^2 - k_{\rm tr}^2)\Big]\exp\Big(ik_{\rm long}\rho - i\,\frac{\pi}{4}\Big),$$

$$U_{\rm tr} = \sqrt{\frac{2\pi}{k_{\rm tr}\rho}}\,\frac{\cos^2\omega}{k_{\rm long}^3 D_{\rm tr}}\Big[\Big(p\,\frac{2k_{2x}^2 - k_{\rm tr}^2}{k_{\rm tr}\sin\omega - k_{2x}} - \frac{2k_{1x}\sqrt{k_{\rm long}^2 - k_{1x}^2}}{k_{\rm tr}\sin\omega - k_{1x}}\Big)2k_{\rm R}\sqrt{k_{\rm R}^2 - k_{\rm tr}^2}$$

$$+\Big(p\,\frac{2k_{2x}\sqrt{k_{\rm tr}^2 - k_{2x}^2}}{k_{\rm tr}\sin\omega - k_{2x}} + \frac{2k_{1x}^2 - k_{\rm tr}^2}{k_{\rm tr}\sin\omega - k_{1x}}\Big)(2k_{\rm R}^2 - k_{\rm tr}^2)\Big]\exp\Big(ik_{\rm tr}\rho - i\,\frac{\pi}{4}\Big).$$

Here $D_{\rm long} = 4\sin^2\omega\cos^2\omega\sqrt{\sin^2\omega - \varepsilon^2} - (2\sin^2\omega - 1)^2$, $D_{\rm tr} = 4\sin^2\omega\cos^2\omega\sqrt{\sin^2\omega - \varepsilon^2} - (2\sin^2\omega - \varepsilon^2)^2$, $\varepsilon = c_{\rm long}/c_{\rm tr}$, and ω is the azimuth angle counted from the z axis.

Figure 4 shows the displacement amplitudes of volume waves U normalized by the shear wave amplitude (curves 1 and 2 refer to longitudinal and transverse waves, respectively). The maximum amplitude of the spatial waves is reached for a wedge angle $\beta = 180^\circ - \theta \approx 120^\circ$. If the refraction process is treated as transition of the energy of the incident Rayleigh wave to surface and spatial waves, then, according to the energy conservation law, a decrease in the energy of diffracted surface waves should lead to an increase in the contribution of volume waves. The experimental data of [1] suggest that for $\beta \approx 120^\circ$, the refraction coefficients are minimal.

Figure 5 shows the distributions of the amplitudes of longitudinal waves (a) and transverse waves (b) over the angle ω (curves 1–4 refer to $\beta = 150$, 140, 120, and 100°, respectively). A comparison of the curves in Figs. 4 and 5 shows that for ω close to 30°, the displacement level is high. A decrease in the wedge angle results in a change in the wave displacement amplitude and a small shift of the maximum of the curve of the amplitude versus the angle ω.

In solving the problem of diffraction over a wedge with a small wedge angle, one should take into account the variation of the incident wave velocity with approach to the wedge angle [5].

The method proposed allows one to study diffraction in the case of more complex diffractors, for example, those with a flat plane.

REFERENCES

1. I. A. Viktorov, *Physics of Application of Rayleigh and Lamb Ultrasonic Waves* [in Russian], Nauka, Moscow (1966).
2. J. Kane and J. Spence, "Rayleigh wave transmission in elastic wedge," *Geophysics*, **28**, No. 5, 715–723 (1963).
3. L. M. Brekhovskikh and V. V. Goncharov, *Introduction to the Mechanics of Continuous Media* [in Russian], Nauka, Moscow (1982).
4. Kh. B. Tolipov and S. Yu. Gurevich, "Special features of diffraction of Rayleigh waves by a wedge," in: *Control of Technologies, Articles, and Environment Using Physical Methods*: Proc. XX Ural Conf. (May 15–16, 2001), Inst. Phys. Met., Ural Div., Russian Acad. of Sci., Ekaterinburg (2001), p. 68.
5. Kh. B. Tolipov, "Dynamic problem of the theory of elasticity for angular regions with homogeneous boundary conditions," *Prikl. Matem. Mekh.*, **57**, No. 5, 120–126 (1993).